



Scan to know paper details and  
author's profile

# Modeling Analysis of a SEIQR Epidemic Model to Assess the Impact of Undetected Cases and Containment Measures of the COVID-19 Outbreak in Cameroon

*L. Nkague Nkamba, M. L. Mann Manyombe, T. T. Manga & J. Mbang*

*University of Yaounde I*

## ABSTRACT

COVID-19 is a highly contagious disease, and the strain is severe acute respiratory syndrome coronavirus 2 (SARS-CoV-2). It belongs to the coronavirus family, which can result in benign diseases in humans, such as a cold, and can also cause serious pathologies such as Severe Acute Respiratory Syndrome (SARS). In this study, we have modeled the COVID-19 epidemic in Cameroon. We used early reported case data to predict the peak, assess the impact of containment measures, and the impact of undetected infected people on the epidemic trend and characteristics of COVID-19. The basic reproduction number is computed using Lyapunov functions, and the global stability of disease-free and endemic equilibrium are demonstrated.

**Keywords:** COVID-19, lyapunov function, global stability, control, peak, SARS- CoV-2 coronavirus.

**Classification:** FOR Code: 321020p

**Language:** English



London  
Journals Press

LJP Copyright ID: 925632  
Print ISSN: 2631-8490  
Online ISSN: 2631-8504

London Journal of Research in Science: Natural and Formal

Volume 20 | Issue 4 | Compilation 1.0





# Modeling Analysis of a SEIQR Epidemic Model to Assess the Impact of Undetected Cases and Containment Measures of the COVID-19 Outbreak in Cameroon

L. Nkague Nkamba <sup>α</sup>, M. L. Mann Manyombe <sup>σ</sup>, T. T. Manga <sup>ρ</sup> & J. Mbang <sup>ω</sup>

## ABSTRACT

*COVID-19 is a highly contagious disease, and the strain is severe acute respiratory syndrome coronavirus 2 (SARS-CoV-2). It belongs to the coronavirus family, which can result in benign diseases in humans, such as a cold, and can also cause serious pathologies such as Severe Acute Respiratory Syndrome (SARS). In this study, we have modeled the COVID-19 epidemic in Cameroon. We used early reported case data to predict the peak, assess the impact of containment measures, and the impact of undetected infected people on the epidemic trend and characteristics of COVID-19. The basic reproduction number is computed using Lyapunov functions, and the global stability of disease-free and endemic equilibrium are demonstrated.*

**Keywords:** COVID-19, lyapunov function, global stability, control, peak, SARS- CoV-2 coronavirus.

**Author α:** Department of Mathematics, Higher Teacher Training College, University of Yaounde I, Yaounde, Cameroon.

**σ:** Department of Mathematics, Faculty of Science, University of Yaounde I, P.O. Box 812 Yaounde, Cameroon.

**ρ:** AIDEPY Association des Ingnieurs Diploms de l'Ecole Polytechnique de Yaound, Cameroon.

## Sources data

We collected the daily numbers of laboratory-confirmed COVID-19 active cases, deaths, and recovered patients, released by the Cameroon Health Emergency Operations Center, from March 6, 2020 to May 4, 2020, to construct a real-time database.

## I. INTRODUCTION

Departing from China in Wuhan on December 31, 2019, the coronavirus epidemic rapidly spread worldwide. After three months of the pandemic, 185 countries were affected [22]. As of April 12, 2020, the world has recorded 1.9 million confirmed cases, with more than 120,000 deaths. Italy [25], France, the United States, and Spain pay the heaviest price in this pandemic. As of April 14, 2020, France reported more than 15,000 deaths, Spain reported more than 18,000, Italy reported more than 20,000, and the United States reported more than 23,000 deaths. As the world entered its sixteenth epidemiological week, the pandemic has become a public health problem for each affected country. Cameroon is one of the most affected countries in Africa, with nearly 1,000 cases confirmed as of April 15, 2020. COVID-19 is a highly contagious disease, and the strain is SARS-CoV-2 [26]. It belongs to the coronavirus family, which can cause benign diseases in humans, such as a cold, and can also cause serious pathologies such as Severe Acute Respiratory Syndrome (SARS). The SARS-CoV-2 coronavirus is not only transmitted from animals to humans but also from humans to humans. The environment is a significant transmission factor; the contact of the hands with infected surfaces, and then with the mouth, nose, and/or eyes can spread the disease. The average incubation time is 5 days, but it can last from 12 to 14 days [15,16]. The most common symptoms are a high fever

and cough. Some people may have headaches and body aches. In severe cases, the infection can cause respiratory distress. Some people do not develop symptoms but remain contagious. The virus is new; there is no proven treatment protocol, nor is a COVID-19 vaccine currently available. The coronavirus mortality rate varies from 2 to 5% from one country to another [12]. After two confirmed cases (01 imported and 01 other contaminated) in Yaound on March 06, 2020, the Minister of Public Health activated the system management of public health emergencies. Subsequently, the escalation of the outbreak in the world sparked the return of several exposed people to Cameroon. The submerged entry device was only able to capture a few cases. The government has taken a series of measures to reduce the spread of COVID-19. More than 13 measures have been implemented throughout the country since March 18, 2020, with the key points being the closure of all maritime and land air borders, the closure of public and private schools and universities until further notice and the systematic quarantine of passengers arriving at the international airports of Douala and Yaound. However, the number of new confirmed cases in Yaound, Bafoussam, and Douala continues to increase (820 total cases recorded, including active cases), and the restriction of work causes a huge impact on society and the Cameroonian economy.

To this end, it is important to have a good understanding of the governing process. As part of the necessary multidisciplinary research approach, mathematical models have been extensively used to provide a framework for understanding COVID-19 transmission dynamics and control strategies of the infection spread in the host population. Mathematical modeling provides an interesting tool for experts to improve disease control strategies. As recognized by WHO, mathematical models, especially those designed in a timely fashion, can play a key role in providing factual information to decision-makers. Modeling can indeed help better understand: (i) transmissibility of the disease; (ii) the time when the number of infected was highest during the epidemic; (iii) impact of some key parameters in the spread of disease; (iv) the severity of the infection; (v) how interventions have been and should be effective.  $R_0$  is an indication of the transmissibility of a virus, representing the average number of new infections generated by an infectious person in a totally naive population. For  $R_0$ , the number infected is likely to increase, and for  $R_0 < 1$ , the transmission is likely to die out. The basic reproduction number is a central concept in infectious disease epidemiology, indicating the risk of an infectious agent with respect to epidemic spread [17]. Considerable works can be found regarding the estimation of the reproductive number of novel coronavirus COVID-19 [17,33]. Liu et al. identified 12 studies that estimated the basic reproductive number for COVID-19 from China and overseas. The period covered was from January 1, 2020, to February 7, 2020. They found that the  $R_0$  was between 1.4 to 6.49. Several models have been used to understand the spread of COVID-19 better. According to Kathakali Biswas et al., the cumulative data can fit into an empirical form obtained from a Susceptible-Infected-Removed (SIR) model studied on a Euclidean network previously [6]. Wu et al. [8,20] introduced a susceptible-exposed-infectious-recovered SEIR model to describe the transmission dynamics. The Chayu et al. model describes the multiple transmission pathways in the infection dynamics and emphasizes the role of the environmental reservoir in the transmission and spread of this disease [29,30]. Some models are used to estimate the transmissivity and mortality of COVID-19 [31,32]. Some papers assessed governmental strategies as isolation of cases and contacts and quarantine [2,11]. Some of them covered the prediction of the peak [13,14,24]. The spread and control of COVID-19 in Australia was studied by Chang et al. [7]. Dashraath et al. found that pregnant women and their fetuses represent a high-risk population during infectious disease outbreaks [8]. Some authors have studied the impact of climate on the spread of COVID-19 [27,28]. Luo et al. discussed the role of absolute humidity on transmission rates of the COVID-19 outbreak [18]. Baud et al.

showed real estimates of mortality following COVID-19 infection [3]. Zoltan et al. Studied COVID-19 epidemic outcome predictions based on logistic fitting and estimation of its reliability.

In this paper, we present a dynamic model for the transmission of COVID-19 in Cameroon, and assess the impact of containment measures and undetected infected people on the epidemic trend and characteristics of COVID-19. The model is based on  $S, E, I_{nd}, I_d, Q, R$  compartments, that are the susceptible compartment ( $S$ ), exposed compartment (individuals in incubation period) ( $E$ ), compartment of undetected infectious ( $I_{nd}$ ), detected infectious compartment ( $I_d$ ), quarantined individuals compartment ( $Q$ ), and removed compartment ( $R$ ), respectively. Using Lyapunov-LaSalle methods, we fully resolve the global dynamics of the model for the full parameter space. We demonstrate that the model exhibits threshold behavior with a globally stable disease-free equilibrium if the basic reproduction number is less than unity and a globally stable endemic equilibrium if the basic reproduction number is greater than unity. In order to study the stability of a positive endemic equilibrium state, we use Lyapunov's direct method and LaSalle's Invariance Principle with a Lyapunov function of Goh-Volterra type:

$$V(x_1, x_2, \dots, x_n) = \sum_i A_i (x_i - x_i^* \ln x_i),$$

where  $A_1, \dots, A_n$  are constants,  $x_i$  is the population of  $i$ th compartment, and  $x_i^*$  is the equilibrium level. Lyapunov functions of this type have also proven to be useful for Lotka–Volterra predator–prey systems [4], and it appears that they can be useful for a more complex compartmental epidemic.

The manuscript is organized as follows. In the next section, we formulate the model and derive its basic properties. In Section 3, we present a mathematical analysis where the reproduction number is derived, the stability of disease-free equilibrium (DFE) is established, and the existence, uniqueness, and stability of an endemic equilibrium are shown. While Section 4 is devoted to numerical simulations conducted using data collected at the Cameroon Health Emergency Operation Center (COUS) from March 6, 2020, to April 14, 2020. Section 5 concludes the paper and provides a discussion for future and ongoing works.

## II. MODEL FORMULATION

In this section, we propose a compartmental model based on the diseases clinical progression and the epidemiological status of individuals. Specifically, the population is subdivided into several compartments, namely: the susceptible compartment ( $S$ ), exposed compartment (individuals in incubation period) ( $E$ ), compartment of undetected infectious ( $I_{nd}$ ), detected infectious compartment ( $I_d$ ), quarantined individuals compartment ( $Q$ ), and removed compartment ( $R$ ). Our model includes a net inflow of susceptible individuals into the region at a rate of  $\lambda$  per unit time. This parameter includes new births, immigration, and emigration. The susceptible population is reduced by containment rate  $c_f$ . Moreover, the susceptible population decreases after infection, acquired through interaction between a susceptible individual and an undetected infected person (at a rate of  $\beta_1$ ) or detected infected person (at a rate of  $\beta_2$ ). A newly infected susceptible individual from group  $S$  becomes an exposed individual, and the rate of infection is given by  $\beta_1 I_{nd} + \beta_2 I_d$ , where  $\beta_1, \beta_2$  are the rate of transmission of compartments  $I_{nd}$  and  $I_d$ , respectively. Exposed individuals are infected individuals but not infectious for the community. Once exposed, individuals progress through the undetected infectious and detected infectious stages with an average  $\delta$ . A fraction  $p$  ( $0 \leq p \leq$

1) of exposed individuals progress to the undetected infectious stage, while a fraction  $1 - p$  of exposed individuals progress to the detected infectious stage.  $\mu$  is the disease-caused death rate for  $I_{nd}$ ,  $I_d$ , and  $Q$  compartments. After a screening, undetected infectious individuals are quarantined at a rate of  $\alpha$ . The recovery rate of undetected infectious individuals is  $\sigma_1$ . Detected infectious individuals are quarantined at a rate  $\varepsilon$ .  $\sigma_2$  is the recovery rate of quarantined individuals. The above-mentioned biological descriptions lead to the following system of nonlinear differential equations whose flow diagram, state variables, and parameters are displayed in Figure1 and Table1, respectively.

$$\begin{cases} \dot{S} &= \lambda - (\beta_1 I_{nd} + \beta_2 I_d)S - c_f S, \\ \dot{E} &= (\beta_1 I_{nd} + \beta_2 I_d)S - \delta E, \\ \dot{I}_{nd} &= p\delta E - (\sigma_1 + \alpha + \mu)I_{nd}, \\ \dot{I}_d &= (1-p)\delta E - (\varepsilon + \mu)I_d, \\ \dot{Q} &= \varepsilon I_d + \alpha I_{nd} - (\sigma_2 + \mu)Q, \\ \dot{R} &= \sigma_1 I_{nd} + \sigma_2 Q, \end{cases} \quad (2.1)$$

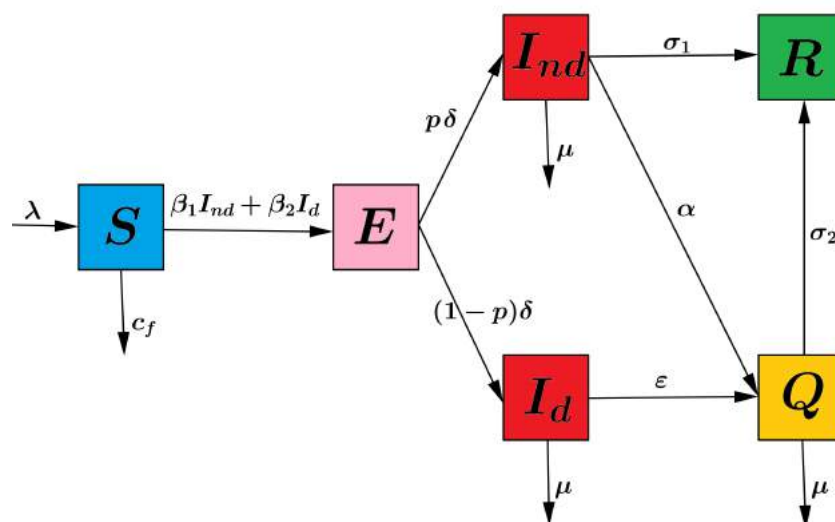


Figure 1: Scheme of the compartmental model

Table 1: Description of state variables and parameters of model (2.1).

Variables	Description
$S$	Susceptible individuals
$E$	Exposed individuals
$I_{nd}$	Undetected infectious individuals
$I_d$	Detected infectious individuals
$Q$	Quarantined individuals
$R$	Recovered individuals

Parameters	Description	Values (Range)	Source
$\lambda$	Recruitment of susceptible individuals	500 (250,1000)	Assumed
$\beta_1$	Transmission rate of undetected infectious individuals	0.001 ( $10^{-5}$ , $5 \times 10^{-3}$ )	Estimated
$\beta_2$	Transmission rate of detected infectious individuals	0.0001 ( $10^{-6}$ , $5 \times 10^{-3}$ )	Estimated
$c_f$	Containment rate of susceptible individuals	variable (0, 1)	Assumed
$\delta$	Incubation rate	1/7 (1/14, 1/2)	[23]
$p$	Fraction of exposed who become undetected infectious	0.8262 (0, 1)	Estimated
$\mu$	Disease induced mortality rate	0.05 (0.03, 0.07)	[1]
$\sigma_1$	Recovery rate of undetected infectious individuals	1/15 (1/17, 1/12)	[23]
$\sigma_2$	Recovery rate of quarantined individuals	1/15 (1/17, 1/12)	[23]
$\alpha$	Quarantined rate of undetected infectious individuals	variable (0, 1)	Assumed
$\varepsilon$	Quarantined rate of detected infectious individuals	variable (0, 1)	Assumed

### III. MATHEMATICAL ANALYSIS

#### 3.1 Basic properties

For the COVID-19 transmission model (2.1) to be epidemiologically meaningful, it is important to prove that all state variables are non-negative at all times. That is, solutions of the system (2.1) with non-negative initial data will remain non-negative for all time  $t > 0$ .

**Theorem 3.1** *Let the initial data be  $S(0)$ ,  $E(0)$ ,  $I_{nd}(0)$ ,  $I_d(0)$ ,  $Q(0)$ ,  $R(0)$  be non-negative. Then, the solutions  $(S, E, I_{nd}, I_d, Q, R)$  of model (2.1) are positive and bounded for all  $t > 0$ , whenever they exist.*

**Proof :** Suppose  $S(0) \geq 0$ . The first equation of system (2.1) can be written as:

$$\frac{d}{dt}[S(t)\rho(t)] = \lambda\rho(t)$$

where  $\rho(t) = \exp\left(\int_0^t [\beta_1 I_{nd}(s) + \beta_2 I_d(s) + c_f] ds\right) > 0$  is the integrating factor. Hence, integrating this last relation with respect to  $t$ , we have

$$S(t)\rho(t) - S(0) = \int_0^t \lambda\rho(s) ds,$$

so that the division of both side by  $\rho(t)$  yields

$$S(t) = \left[ S(0) + \int_0^t \lambda\rho(s) ds \right] \times \rho^{-1}(t) > 0.$$

The same arguments can be used to prove that  $E(t) > 0$  and  $I_{nd}(t)$ ,  $I_d(t)$ ,  $Q(t)$ ,  $R(t) \geq 0$  for all  $t > 0$ .



where  $d_0 = \min\{c_f, \mu\}$ . This implies that

$$\lim_{t \rightarrow +\infty} \sup N(t) \leq \frac{\lambda}{d_0}.$$

Further, from (2.1), we have  $\dot{S} \leq \lambda - c_f S$ . Thus,  $\lim_{t \rightarrow +\infty} \sup S(t) \leq \frac{\lambda}{d_0}$ . This completes the proof.

Combining Theorem 3.1 with the trivial existence and uniqueness of a local solution for the model (2.1), we have established the following theorem which ensures the mathematical and biological well-posedness of the system (2.1).

**Theorem 3.2** *The dynamics of model (2.1) represent a dynamical system in the biological feasible compact set*

$$\Gamma = \left\{ (S, E, I_{nd}, I_d, Q, R) \in \mathbb{R}_+^6 : 0 \leq S \leq \frac{\lambda}{c_f}, \quad N \leq \frac{\lambda}{d_0} \right\}.$$

The first four equations of model (2.1) are independent of the states  $Q$  and  $R$ . Consequently, after decoupling the equations for  $Q$  and  $R$  from model (2.1), we devote the analysis to the remaining equations of system (2.1) which becomes

$$\begin{cases} \dot{S} &= \lambda - (\beta_1 I_{nd} + \beta_2 I_d)S - c_f S, \\ \dot{E} &= (\beta_1 I_{nd} + \beta_2 I_d)S - \delta E, \\ \dot{I}_{nd} &= p\delta E - (\sigma_1 + \alpha + \mu)I_{nd}, \\ \dot{I}_d &= (1-p)\delta E - (\varepsilon + \mu)I_d. \end{cases} \quad (3.1)$$

It is easy to check that model (3.1) always has a disease-free equilibrium  $P_0 = (S_0, 0, 0, 0)$  where  $S_0 = \frac{\lambda}{c_f}$ , which is obtained by setting the right-hand side of system (3.1) to zero.

A key quantity in classic epidemiological models is the basic reproduction number, denoted by  $R_0$ . It is a useful threshold in the study of a disease for predicting a disease outbreak and for evaluating the control strategies. Following [9], the next-generation approach is used to calculate  $R_0$ . Let

$$\mathcal{F} = \left( \beta_1 S I_{nd} + \beta_2 I_d, p\delta E, (1-p)\delta E \right)^T \quad \text{and} \quad \mathcal{V} = \left( -\delta E, -(\sigma_1 + \mu + \alpha)I_{nd}, -(\mu + \varepsilon)I_d \right)^T,$$

be the vector of new generated infected and the vector of transfers between compartments, respectively. The Jacobian matrices of  $\mathcal{F}$  and  $\mathcal{V}$  at the DFE  $P_0$  are

$$F = \begin{pmatrix} 0 & \beta_1 S_0 & \beta_2 S_0 \\ p\delta & 0 & 0 \\ (1-p)\delta & 0 & 0 \end{pmatrix} \quad \text{and} \quad V = \begin{pmatrix} -\delta & 0 & 0 \\ 0 & -(\sigma_1 + \mu + \alpha) & 0 \\ 0 & 0 & -(\mu + \varepsilon) \end{pmatrix}.$$



From the conclusion by [9], the associated basic reproduction number  $\mathcal{R}_0$  of (3.1) is the spectral radius of the next-generation matrix  $-FV^{-1}$ . That is

$$\mathcal{R}_0 = \sqrt{\frac{\lambda}{c_f} \left( \frac{p\beta_1}{\sigma_1 + \mu + \alpha} + \frac{(1-p)\beta_2}{\mu + \varepsilon} \right)}, \quad (3.2)$$

$$\mathcal{R}_0^2 = \frac{\lambda p \beta_1}{c_f(\sigma_1 + \mu + \alpha)} + \frac{\lambda(1-p)\beta_2}{c_f(\mu + \varepsilon)} \quad (3.3)$$

$$\mathcal{R}_0^2 = \mathcal{R}_{Ind} + \mathcal{R}_{Id} \quad (3.4)$$

which represents the average number of secondary COVID-19 infections. In fact,  $\mathcal{R}_{Ind} = \frac{\lambda p \beta_1}{c_f(\sigma_1 + \mu + \alpha)}$  is the average number of secondary infections caused by an undetected infectious individual, while  $\mathcal{R}_{Id} = \frac{\lambda(1-p)\beta_2}{c_f(\mu + \varepsilon)}$  is the average number of secondary infections caused by a detected infectious individual. When  $p$  is near to unity, the weight of  $\mathcal{R}_0$  is greatly impacted by undetected infectious individual

The infected population can be effectively controlled if  $\mathcal{R}_0 < 1$ . To ensure that the effective control of the infected population is independent of the initial size of the human population, a global asymptotic stability result must be established for the DFE.

**Theorem 3.3** *If  $\mathcal{R}_0 \leq 1$ , then the disease-free equilibrium is globally asymptotically stable.*

*Proof :* Let  $X = (S, E, I_{nd}, I_d)^T$  and consider a Lyapunov function,

$$\mathcal{V}(X) = E + \frac{\beta_1 S_0}{\sigma_1 + \alpha + \mu} I_{nd} + \frac{\beta_2 S_0}{\varepsilon + \mu} I_d.$$

Direct calculation leads to

$$\begin{aligned} \dot{\mathcal{V}} &= \dot{E} + \frac{\beta_1 S_0}{\sigma_1 + \alpha + \mu} \dot{I}_{nd} + \frac{\beta_2 S_0}{\varepsilon + \mu} \dot{I}_d, \\ &= (\beta_1 I_{nd} + \beta_2 I_d)S - \delta E + \frac{\beta_1 S_0}{\sigma_1 + \alpha + \mu} (p\delta E - (\sigma_1 + \alpha + \mu)I_{nd}) + \frac{\beta_2 S_0}{\varepsilon + \mu} ((1-p)\delta E - (\varepsilon + \mu)I_d) \\ &= (\beta_1 I_{nd} + \beta_2 I_d)(S - S_0) + \left( \frac{p\beta_1 S_0}{\sigma_1 + \alpha + \mu} + \frac{(1-p)\beta_2 S_0}{\varepsilon + \mu} - 1 \right) \delta E \end{aligned}$$

Since  $S \leq S_0$ , we have

$$\dot{\mathcal{V}} \leq \delta(\mathcal{R}_0^2 - 1)E \leq 0 \quad \text{whenever} \quad \mathcal{R}_0 \leq 1.$$

Furthermore,

$$\dot{\mathcal{V}} = 0 \Leftrightarrow E = 0, I_{nd} = 0, I_d = 0 \quad \text{or} \quad S = S_0 \text{ and } \mathcal{R}_0 = 1.$$

Thus, the largest invariant set  $\mathcal{H}$  such as  $\mathcal{H} \subset \{X \in \Omega / \dot{\mathcal{V}}(X) = 0\}$  is the singleton  $\{P_0\}$ . By LaSalle's Invariance Principle,  $P_0$  is globally asymptotically stable in  $\Gamma$ , completing the proof.

### 3.3 Endemic equilibrium and its stability

An equilibrium  $P^* = (S^*, E^*, I_{nd}^*, I_d^*)$  of model 3.1 must satisfy the following equations:

$$\begin{cases} \lambda - \beta_1 S^* I_{nd}^* - \beta_2 S^* I_d^* - c_f S^* &= 0, \\ \beta_1 S^* I_{nd}^* + \beta_2 S^* I_d^* - \delta E^* &= 0, \\ p\delta E^* - (\sigma_1 + \alpha + \mu) I_{nd}^* &= 0, \\ (1-p)\delta E^* - (\varepsilon + \mu) I_d^* &= 0. \end{cases} \quad (3.5)$$

Solving (3.5) for  $P^*$  yields

$$S^* = \frac{\lambda}{\beta_1 I_{nd}^* + \beta_2 I_d^* + c_f}, \quad I_{nd}^* = \frac{p\delta E^*}{\sigma_1 + \alpha + \mu}, \quad I_d^* = \frac{(1-p)\delta E^*}{\varepsilon + \mu}. \quad (3.6)$$

By adding the two first equations of (3.5), we obtain

$$\lambda - c_f S^* - \delta E^* = 0 \quad (3.7)$$

After substituting (3.6) into (3.7), we obtain the following equation for  $E^*$

$$-\frac{\delta c_f \mathcal{R}_0^2}{\lambda} (E^*)^2 + c_f (\mathcal{R}_0^2 - 1) E^* = 0, \quad (3.8)$$

from which, we have  $E^* = \frac{\lambda}{\delta} \left(1 - \frac{1}{\mathcal{R}_0^2}\right)$ .

Substituting the expression of  $E^*$  in (3.6), we have

$$S^* = \frac{\lambda}{c_f \mathcal{R}_0^2}, \quad I_{nd}^* = \frac{p\lambda}{\sigma_1 + \alpha + \mu} \left(1 - \frac{1}{\mathcal{R}_0^2}\right), \quad I_d^* = \frac{(1-p)\lambda}{\varepsilon + \mu} \left(1 - \frac{1}{\mathcal{R}_0^2}\right),$$

which exist whenever  $R_0 > 1$ .

We further establish that all solutions in the interior of the feasible region converge to the unique endemic equilibrium  $P^*$  if  $R_0 > 1$ . Therefore, COVID-19 will persist at the endemic equilibrium level. The proof is accomplished by constructing a global Lyapunov function. Lyapunov functions of Goh–Volterra type have been used in the literature (see [10,19]).

**Theorem 3.4** *If  $R_0 > 1$ , then the endemic equilibrium point  $P^* = (S^*, E^*, I_{nd}^*, I_d^*)$  is globally asymptotically stable in  $\Gamma$ .*

**Proof:** We know that the endemic equilibrium  $P^*$  for system 3.1 satisfies the following equalities:

$$\begin{aligned} \lambda &= (\beta_1 I_{nd}^* + \beta_2 I_d^*) S^* + c_f S^*, \\ (\beta_1 I_{nd}^* + \beta_2 I_d^*) S^* &= \delta E^*, \\ p\delta E^* &= (\sigma_1 + \alpha + \mu) I_{nd}^*, \\ (1-p)\delta E^* &= (\varepsilon + \mu) I_d^*. \end{aligned} \quad (3.9)$$

Let  $X = (S, E, I_{nd}, I_d)^T \in \mathbb{R}_+^4$  and consider the following candidate Lyapunov function

$$\begin{aligned} \mathcal{V}_1(x) = & \left( S - S^* - S^* \ln \frac{S}{S^*} \right) + \left( E - E^* - E^* \ln \frac{E}{E^*} \right) \\ & + b_1 \left( I_{nd} - I_{nd}^* - I_{nd}^* \ln \frac{I_{nd}}{I_{nd}^*} \right) + b_2 \left( I_d - I_d^* - I_d^* \ln \frac{I_d}{I_d^*} \right), \end{aligned}$$

where

$$b_1 = \frac{\beta_1 S^*}{\sigma_1 + \alpha + \mu} \quad \text{and} \quad b_2 = \frac{\beta_2 S^*}{\varepsilon + \mu}.$$

Note that  $\mathcal{V}_1(x) \geq 0$  for  $x \in \text{Int}\Gamma$ , the interior of  $\Gamma$ . Thus, function  $\mathcal{V}_1$  is positive definite with respect to the endemic equilibrium  $P^*$ .

Differentiating  $\mathcal{V}_1(X)$  with respect to time yields:

$$\begin{aligned} \dot{\mathcal{V}}_1 = & \left( 1 - \frac{S^*}{S} \right) \dot{S} + \left( 1 - \frac{E^*}{E} \right) \dot{E} + b_1 \left( 1 - \frac{I_{nd}^*}{I_{nd}} \right) \dot{I}_{nd} + b_2 \left( 1 - \frac{I_d^*}{I_d} \right) \dot{I}_d, \\ = & \left( 1 - \frac{S^*}{S} \right) (\lambda - (\beta_1 I_{nd} + \beta_2 I_d)S - c_f S) + \left( 1 - \frac{E^*}{E} \right) ((\beta_1 I_{nd} + \beta_2 I_d)S - \delta E) \\ & + b_1 \left( 1 - \frac{I_{nd}^*}{I_{nd}} \right) (p\delta E - (\sigma_1 + \alpha + \mu)I_{nd}) + b_2 \left( 1 - \frac{I_d^*}{I_d} \right) ((1-p)\delta E - (\varepsilon + \mu)I_d). \end{aligned}$$

Developing and using the first relation of (3.9), we obtain

$$\begin{aligned} \dot{\mathcal{V}}_1 = & c_f S^* \left( 2 - \frac{S^*}{S} - \frac{S}{S^*} \right) + (\beta_1 I_{nd}^* + \beta_2 I_d^*) S^* + \delta E^* + b_1 (\sigma_1 + \alpha + \mu) I_{nd}^* + b_2 (\varepsilon + \mu) I_d^* \\ & - (\beta_1 I_{nd}^* + \beta_2 I_d^*) \frac{(S^*)^2}{S} - (\beta_1 I_{nd} + \beta_2 I_d) \frac{S E^*}{E} - b_1 p \delta E \frac{I_{nd}^*}{I_{nd}} - b_2 (1-p) \delta E \frac{I_d^*}{I_d} \end{aligned}$$

Replacing  $b_1$  and  $b_2$  by their values and exploiting relations (3.9), we have

$$b_1 p \delta = \frac{\beta_1 S^* I_{nd}^*}{E^*} \quad \text{and} \quad b_2 (1-p) \delta = \frac{\beta_2 S^* I_d^*}{E^*}. \quad (3.10)$$

Thus, using relations (3.9) and (3.10), we obtain

$$\begin{aligned} \dot{\mathcal{V}}_1 = & c_f S^* \left( 2 - \frac{S^*}{S} - \frac{S}{S^*} \right) + 3(\beta_1 I_{nd}^* + \beta_2 I_d^*) S^* - (\beta_1 I_{nd}^* + \beta_2 I_d^*) \frac{(S^*)^2}{S} \\ & - (\beta_1 I_{nd} + \beta_2 I_d) \frac{S E^*}{E} - \beta_1 S^* I_{nd}^* \frac{E I_{nd}^*}{E^* I_{nd}} - \beta_2 S^* I_d^* \frac{E I_d^*}{E^* I_d} \\ = & c_f S^* \left( 2 - \frac{S^*}{S} - \frac{S}{S^*} \right) + \beta_1 I_{nd}^* S^* \left( 3 - \frac{S^*}{S} - \frac{E I_{nd}^*}{E^* I_{nd}} - \frac{S E^* I_{nd}}{S^* E I_{nd}^*} \right) \\ & + \beta_2 I_d^* S^* \left( 3 - \frac{S^*}{S} - \frac{E I_d^*}{E^* I_d} - \frac{S E^* I_d}{S^* E I_d^*} \right). \end{aligned}$$

Finally, using the arithmetic-geometric means inequality,  $n - (a_1 + a_2 + \dots + a_n) \leq 0$ , where  $a_1 \cdot a_2 \cdot \dots \cdot a_n = 1$  and  $a_1, a_2, \dots, a_n > 0$ , it follows that  $\dot{V}_1 \leq 0$ . Furthermore,

$$\dot{V}_1 = 0 \iff (S, E, I_{nd}, I_d) = (S^*, E^*, I_{nd}^*, I_d^*).$$

The global stability of the endemic equilibrium follows from the classical stability theorem of Lyapunov and the LaSalle's Invariance Principle.

## IV. NUMERICAL SIMULATIONS

### 4.1 Model fitting

Though the first confirmed case of COVID-19 was reported on 06<sup>th</sup> March 2020, the new cases are being reported continuously from 17<sup>th</sup> March 2020 onwards,. Therefore, we consider 17<sup>th</sup> March 2020 as the starting date of the outbreak in Cameroon. We set the population size of Yaounde and Douala as the initial value of the susceptible group ( $S(0) = 8e6$ ) since the COVID-19 infectious cases before 17<sup>th</sup> March 2020 were all in these cities. The incubation period of COVID-19 ranges from 2 to 14 days, with a mean of 5 to 7 days [23], and we take the value 7 days in our model. The average recovery period is about 15 days [23], and thus, we set the disease recovery rates as  $\sigma_1 = \sigma_2 = 1/15$  per day.

We fit our model to the daily cumulative new reported COVID-19 cases of Cameroon during the period 17<sup>th</sup> March 2020 to 10<sup>th</sup> April 2020. The daily cumulative case data are obtained from [1]. We estimate three unknown model parameters: (i) the transmission rate of undetected infectious ( $\beta_1$ ), (ii) transmission rate of detected infectious ( $\beta_2$ ), and (iii) fraction of population moved to undetected infectious exposed class ( $p$ ) by fitting the model to the data of cumulative reported cases. We use the least-square method to carry out the parameter estimation, which is implemented by the command *fminsearch* in MATLAB (Mathworks R2013a) to minimize the sum of square function. In our case, the cumulative new reported cases from the model is given by

$$C(t, \Theta) = C(0) + \int_0^t (\alpha I_{nd}(s) + \varepsilon I_d(s)) ds,$$

where  $\Theta = \{\beta_1, \beta_2, p\}$  and  $C(0)$  denotes the initial cumulative cases. The sum of square function  $f(\Theta, n)$  is given by

$$f(\Theta, n) = \sum_{i=1}^n \left( C(t_i, \Theta) - C^d(t_i) \right)^2,$$

where  $C^d(t_i)$  is the actual data value at  $t^{th}$  day and  $n$  is the number of data points.

The model fitting to the cumulative new reported cases is displayed in Figure 2. The values of the estimated parameters are given in Table 1. It is seen from Figure 2 that model (2.1) prediction shows a similar trend to the reported data of the cumulative confirmed cases.

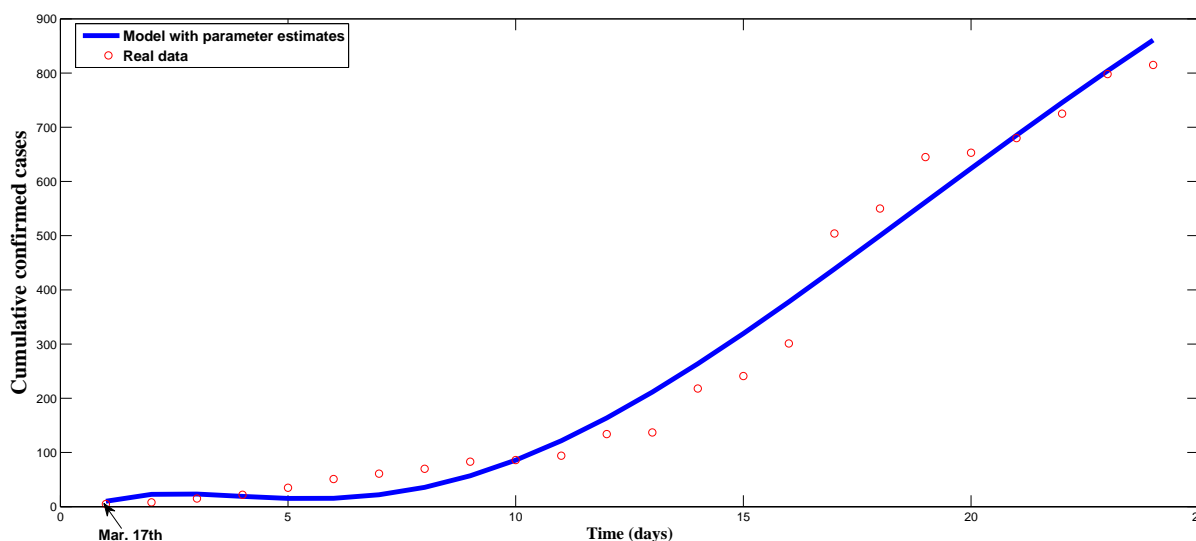


**Figure 2:** Model fitting to cumulative new COVID-19 reported cases for the period 17<sup>th</sup> March 2020 to 10<sup>th</sup> April 2020. The solid blue line represents the model solution and red circles are the discrete data points.

## 4.2 Sensitivity analysis

We carried out a sensitivity analysis to determine the models robustness to parameter values. This is a tool to identify the most influential parameters in determining model dynamics [5]. A Latin Hypercube Sampling (LHS) scheme [21] that samples 1000 values for each input parameter using a uniform distribution over the range of ecologically realistic values is provided in Figure3with descriptions and references in Table1. Using the system of differential equations that describe (2.1), 5000 model simulations were performed by randomly pairing sampled values for all LHS parameters. Partial Rank Correlation Coefficients (PRCC) and corresponding p-values between  $R_0$  and each parameter were computed. An output is assumed sensitive to an input if the corresponding PRCC is less than  $-0.50$  or greater than  $+0.50$ , and the corresponding p-value is less than 5%.

From Figure 3, we can identify parameters that strongly influence the dynamics of COVID-19 infection, namely  $\lambda$ ,  $\beta_1$ ,  $\beta_2$ ,  $c_f$ ,  $\alpha$ , and  $\varepsilon$ . Parameters  $\lambda$ ,  $\beta_1$  and  $\beta_2$  have a positive influence on the basic reproduction number  $R_0$ , that is, an increase in these parameters implies an increase in  $R_0$ . While parameters  $c_f$ ,  $\varepsilon$  and  $\alpha$  have a negative influence on the basic reproduction number  $R_0$ , that is, an increase in these parameters implies a decrease in  $R_0$ . Thus, from this sensitivity analysis, the following suggestions are made:

- The lock-down of borders could be an effective control measure against the growing of COVID-19 infection because it reduces the value of influx rate  $\lambda$ ;

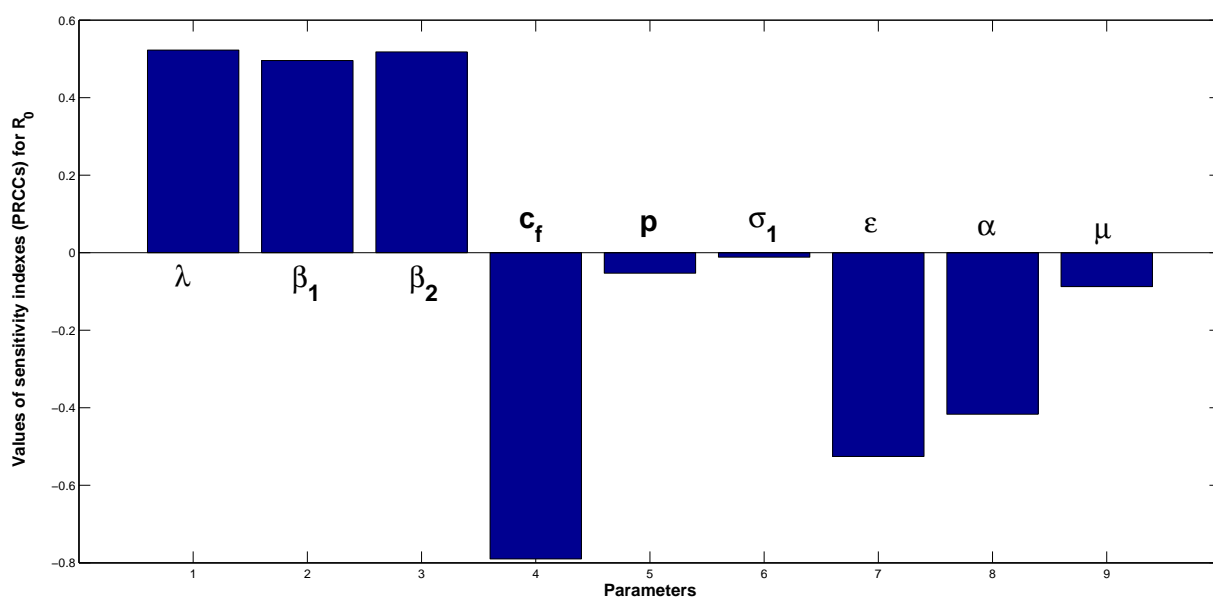


Figure 3: Sensitivity analysis between  $R_0$  and each parameter.

- ii. The containment of susceptible individuals may play an important role in minimizing the size of infected individuals because it helps reduce the values of transmission rates  $\beta_1$  and  $\beta_2$ , and helps increase the value of containment rate  $c_f$ .
- iii. Massive screening is another good control tool against COVID-19 infection because it helps increase the value of quarantined rate  $\alpha$  and helps reduces the value of  $p$ .

#### 4.3 Short-term predictions

We perform numerical simulations in order to examine the short-term predictions of the model (2.1) starting from April 03 (marked as day 0 in these simulations). The parameter values used in this section are listed in Table1.

Figures 4 and 5 display short-term predictions for undetected infectious ( $I_{nd}$ ) and de- tected infectious ( $I_d$ ) in Cameroon using our model. These figures show that the infection level, starting from April 03, would continue increasing, reaching a peak value, and then gradually go down afterward.

To further explore the possible impact of extensive screening on the disease transmis- sion, we plot model (2.1) by varying the values of proportion  $p$  and quarantined rate  $\alpha$ . We first consider the situation where 80% of the exposed individuals become undetected infectious (i.e.,  $p = 0.8$ ). Figure 4 depicts the effect of the proportion of undetected cases ( $p$ ) on disease transmission. From this figure, we see that the peak of the outbreak occurs

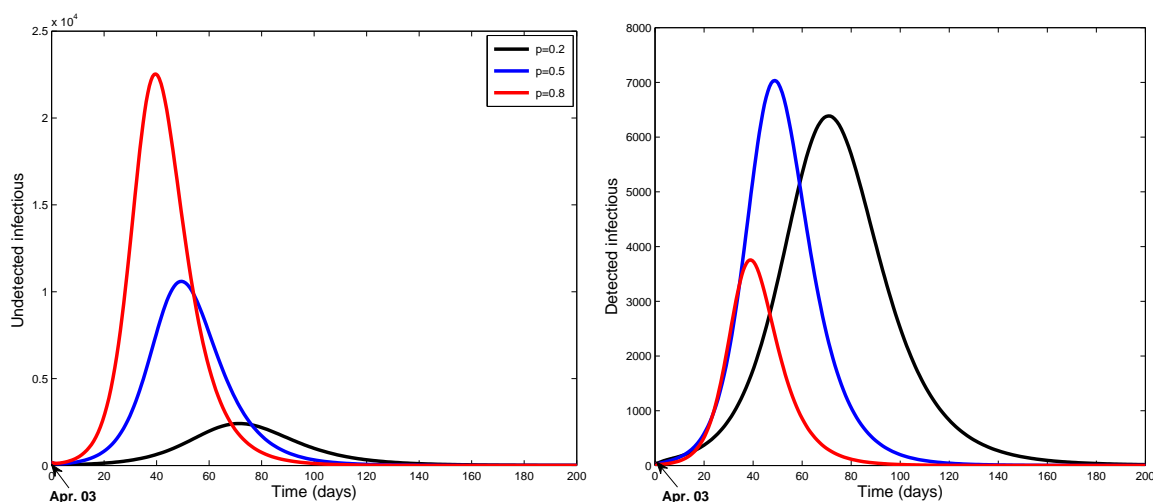


Figure 4: Effect of the proportion  $p$  on disease transmission.

at around 40 days. For the low value of the proportion  $p$  (i.e.,  $p = 0.5$ ), it is observed that the peak of the outbreak is shifted to 50 days, and the peak value of the outbreak is decreased. If the proportion  $p$  is reduced further (i.e.,  $p = 0.2$ ), the peak is shifted to 80 days, and the peak value of the outbreak is further lowered. In summary, with reducing proportion  $p$ , the peak arrives much later, and the peak value is lower.

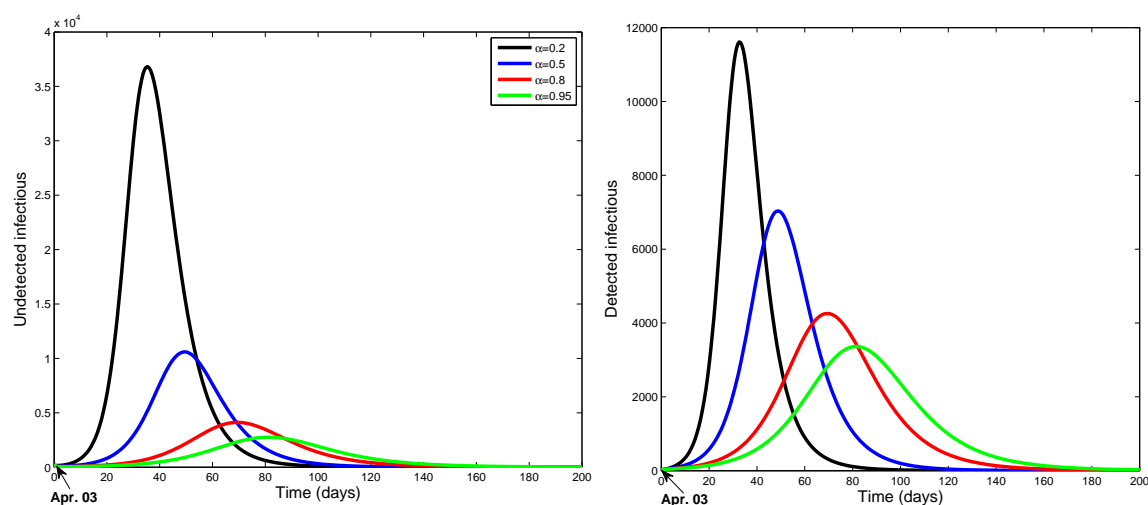


Figure 5: Effect of quarantined rate of undetected infectious on the disease transmission.

Now, we fix the value of proportion  $p = 0.8$  and vary the quarantined rate  $\alpha$ . Figure 5 depicts the effect of the quarantined rate of undetected infectious cases ( $\alpha$ ) on disease transmission. This figure shows that with increasing  $\alpha$ , the peak of the outbreak arrives much later, and the peak value is further lowered.



## V. CONCLUSION AND DISCUSSION

We were pursuing the objective of setting up a compartmental propagation model for COVID-19 and showing the incidence of certain key parameters in the evolution of this disease. The  $SEIQ$   $R$  model led to a sensitivity analysis, which shows a strong dominance of the confinement rate and the quarantine speed over the basic reproduction number  $R_0$ . Considering the situation in Cameroon, with a higher proportion of infected people not detected, a slow quarantine rate will increase the peak of infected people, which will grow with continued delays. Therefore, this study has the merit of exposing the impact of the rate of confinement in the spread of the disease and the need to have capacities in terms of treatment and isolation of patients. Consequently, new ways are opened for better control of undetected infected people, representing 80% of the infected population in our mathematical model, and the strategy to master the confinement of the population.

## ACKNOWLEDGMENTS

The first author thanks the Cameroon Health Emergency Operations Center, Yaounde, Cameroon.

### Disclosure statement

The authors declare no conflict of interest.

## REFERENCES

1. Coronavirus dans le monde et par pays. [http:// coronavirus. politologue. com/ coronavirus-Cameroun. cm](http://coronavirus.politologue.com/coronavirus-Cameroun.cm), accessed : May, 2020.
2. Roy M Anderson, Hans Heesterbeek, Don Klinkenberg, and T D'eirdre Hollingsworth. How will country-based mitigation measures influence the course of the covid-19 epidemic? *The Lancet*, 395(10228):931–934, 2020.
3. David Baud, Xiaolong Qi, Karin Nielsen-Saines, Didier Musso, L'eo Pomar, and Guillaume Favre. Real estimates of mortality following covid-19 infection. *The Lancet infectious diseases*, 2020.
4. E. Beretta and Y. Takeuchi. Global asymptotic stability of Lotka-Volterra diffusion models with continuous time delay. *SIAM Journal on Applied Mathematics*, 48(3):627–651, 1988.
5. T. Berge, S. Bowong, J. Lubuma, and M. L. Mann Manyombe. Modelling ebola virus disease transmissions with reservoir in a complex virus life ecology. *Mathematical Biosciences and Engineering*, 15(1):21–56, 2018.
6. Kathakali Biswas, Abdul Khaleque, and Parongama Sen. Covid-19 spread: Reproduction of data and prediction using a sir model on euclidean network. *arXiv preprint arXiv:2003.07063*, 2020.
7. Sheryl L Chang, Nathan Harding, Cameron Zachreson, Oliver M Cliff, and Mikhail Prokopenko. Modelling transmission and control of the covid-19 pandemic in australia. *arXiv preprint arXiv:2003.10218*, 2020.
8. Pradip Dashraath, Wong Jing Lin Jeslyn, Lim Mei Xian Karen, Lim Li Min, Li Sarah, Arijit Biswas, Mahesh Arjandas Choolani, Citra Mattar, and Su Lin Lin. Coronavirus disease 2019 (covid-19) pandemic and pregnancy. *American Journal of Obstetrics and Gynecology*, 2020.
9. [9]O. Diekmann and J. A. P. Heesterbeek. *Mathematical epidemiology of infectious diseases: model building, analysis and interpretation*, volume 5. John Wiley & Sons, 2000.

10. Hongbin Guo and Michael Y Li. Global stability in a mathematical model of tuber- culosis. *Canadian applied mathematics quarterly*, 14(2), 2006.
11. Joel Hellewell, Sam Abbott, Amy Gimma, Nikos I Bosse, Christopher I Jarvis, Timo- thy W Russell, James D Munday, Adam J Kucharski, W John Edmunds, Fiona Sun, et al. Feasibility of controlling covid-19 outbreaks by isolation of cases and contacts. *The Lancet Global Health*, 2020.
12. Hyungjin Kim. Outbreak of novel coronavirus (covid-19): What is the role of radi- ologists?, 2020.
13. Adam J Kucharski, Timothy W Russell, Charlie Diamond, Yang Liu, John Edmunds, Sebastian Funk, Rosalind M Eggo, Fiona Sun, Mark Jit, James D Munday, et al. Early dynamics of transmission and control of covid-19: a mathematical modeling study. *The lancet infectious diseases*, 2020.
14. Toshikazu Kuniya. Prediction of the epidemic peak of coronavirus disease in japan, 2020. *Journal of Clinical Medicine*, 9(3):789, 2020.
15. Stephen A Lauer, Kyra H Grantz, Qifang Bi, Forrest K Jones, Qulu Zheng, Hannah R Meredith, Andrew S Azman, Nicholas G Reich, and Justin Lessler. The incubation period of coronavirus disease 2019 (covid-19) from publicly reported confirmed cases: estimation and application. *Annals of internal medicine*, 2020.
16. Natalie M Linton, Tetsuro Kobayashi, Yichi Yang, Katsuma Hayashi, Andrei R Akhmetzhanov, Sung-mok Jung, Baoyin Yuan, Ryo Kinoshita, and Hiroshi Nishiura. Incubation period and other epidemiological characteristics of 2019 novel coronavirus infections with right truncation: a statistical analysis of publicly available case data. *Journal of clinical medicine*, 9(2):538, 2020.
17. Ying Liu, Albert A Gayle, Annelies Wilder-Smith, and Joacim Rocklöv. The repro- ductive number of covid-19 is higher compared to sars coronavirus. *Journal of travel medicine*, 2020.
18. Wei Luo, Maimuna Majumder, Dianbo Liu, Canelle Poirier, Kenneth Mandl, Marc Lipsitch, and Mauricio Santillana. The role of absolute humidity on transmission rates of the covid-19 outbreak. 2020.
19. M. L. Mann Manyombe, J. Mbang, J. Lubuma, and B. Tsanou. Global dynamics of a vaccination model for infectious diseases with asymptomatic carriers. *Mathematical Biosciences and Engineering*, 13(4):813–840, 2016.
20. Solym MANOU-ABI and Julien BALICCHI. Analysis of the covid-19 epidemic in french overseas department mayotte based on a modified deterministic and stochastic seir model. *medRxiv*, 2020.
21. S. Marino, I. B. Hogue, C. J. Ray, and D. E. Kirschner. A methodology for performing global uncertainty and sensitivity analysis in systems biology. *Journal of Theoretical Biology*, 254:178–196, 2008.
22. World Health Organization et al. Coronavirus disease 2019 (covid-19): situation report, 72. 2020.
23. Remy Pasco, Xutong Wang, Michaela Petty, Zhanwei Du, Spencer J Fox, Michael Pignone, Clay Johnston, and Lauren Ancel Meyers. Covid-19 healthcare demand projections: Austin, texas, 2020.
24. Liangrong Peng, Wuyue Yang, Dongyan Zhang, Changjing Zhuge, and Liu Hong. Epidemic analysis of covid-19 in china by dynamical modeling. *arXiv preprint arX- iv:2002.06563*, 2020.
25. Andrea Remuzzi and Giuseppe Remuzzi. Covid-19 and italy: what next? *The Lancet*, 2020.

26. Muhammad Adnan Shereen, Suliman Khan, Abeer Kazmi, Nadia Bashir, and Rabeea Siddique. Covid-19 infection: origin, transmission, and characteristics of human coronaviruses. *Journal of Advanced Research*, 2020.
27. Tanu Singhal. A review of coronavirus disease-2019 (covid-19). *The Indian Journal of Pediatrics*, pages 1–6, 2020.
28. Jingyuan Wang, Ke Tang, Kai Feng, and Weifeng Lv. High temperature and high humidity reduce the transmission of covid-19. *Available at SSRN 3551767*, 2020.
29. Thomas P Weber and Nikolaos I Stilianakis. Inactivation of influenza a viruses in the environment and modes of transmission: a critical review. *Journal of infection*, 57(5):361–373, 2008.
30. Chayu Yang and Jin Wang. A mathematical model for the novel coronavirus epidemic in wuhan, china. *Mathematical Biosciences and Engineering*, 17(3):2708–2724, 2020.
31. Shu Yang, Peihua Cao, Peipei Du, Ziting Wu, Zian Zhuang, Lin Yang, Xuan Yu, Qi Zhou, Xixi Feng, Xiaohui Wang, et al. Early estimation of the case fatality rate of covid-19 in mainland china: a data-driven analysis. *Annals of Translational Medicine*, 8(4), 2020.
32. Jing Yuan, Minghui Li, Gang Lv, and Z Kevin Lu. Monitoring transmissibility and mortality of covid-19 in europe. *International Journal of Infectious Diseases*, 2020.
33. Sheng Zhang, MengYuan Diao, Wenbo Yu, Lei Pei, Zhaofen Lin, and Dechang Chen. Estimation of the reproductive number of novel coronavirus (covid-19) and the probable outbreak size on the diamond princess cruise ship: A data-driven analysis. *International Journal of Infectious Diseases*, 93:201–204, 2020.